

## Hydrodynamic modelling of a regulated Mediterranean coastal lagoon, the Albufera of Valencia (Spain)

Javier García Alba, Aina G. Gómez, Pilar del Barrio Fernández,  
Andrés García Gómez and César Álvarez Díaz

### ABSTRACT

Coastal lagoon hydrodynamics are strongly influenced by sea water exchange, especially when the connection between the lagoon and the sea is artificially regulated. These situations increase the complexity of the hydrodynamic regime, requiring the use of numerical models to understand their behaviour. Traditionally, one-dimensional models have been used, although in recent years, the development of two-dimensional shallow water models and advanced numerical techniques have increased notably. However, most of the existing bi-dimensional models consider the connection to the sea as a boundary condition, and they do not take into consideration the sea-lagoon exchange. In this paper, a fully two-dimensional hydrodynamic model of a heavily regulated coastal lagoon, which includes the artificial connection with the sea, is presented. The model allows the characterization of water level variation in the lagoon, taking into account the combined effect of different forcings. This model consists of two hydrodynamic modules: a long wave module (two-dimensional depth-averaged) which includes the analysis of a system of sluice gates, and a wind module (quasi three-dimensional). The model was successfully calibrated and validated with real data, showing its ability to accurately describe the hydraulic dynamics of regulated coastal lagoons.

**Key words** | coastal lagoon, currents, hydraulics, hydrodynamics, modelling, sluice gates

Javier García Alba (corresponding author)  
Aina G. Gómez  
Pilar del Barrio Fernández  
Andrés García Gómez  
César Álvarez Díaz  
Environmental Hydraulics Institute,  
'IH Cantabria',  
Universidad de Cantabria. C/ Isabel Torres  
No. 15. Parque Científico y Tecnológico de  
Cantabria. 39011,  
Santander,  
Spain  
E-mail: garciajav@unican.es

### INTRODUCTION

Hydrodynamic modelling of artificially-connected shallow coastal lagoons is very complex because it must include several factors. For example, differences in water level between the sea and the lagoon will determine the magnitude and direction of the flow through the connection domain. Other factors that should be taken into consideration are water inflows to the coastal lagoon, as well as atmospheric conditions. In this respect, it is noteworthy that modelling the sea-lagoon connection in heavily regulated systems is a fundamental issue, being often incorporated as a boundary condition (Spillman *et al.* 2009). In fact, one-dimensional models are commonly used to study this kind of system (Li *et al.* 1999; Murray & Parslow 1999; Usaquén *et al.* 2012). However, the application of a two-dimensional model would allow for a better description of the spatial

and temporal variability of the system's dynamics (Liang & Molkenthin 2001). Moreover, the regulated connection between the sea and the lagoon could be incorporated within the computational domain and not as a boundary condition. Another aspect that should be taken into account is that although the sea level is mainly conditioned by the astronomical tide, it can also be influenced by meteorological factors (Pasaric & Orlic 2001), as is often the case in Mediterranean coastal lagoons, such as the Albufera of Valencia (Spain).

The Albufera of Valencia is a complex hydrodynamics system located on the Mediterranean coast, 12 km south of the city of Valencia, Spain (del Barrio *et al.* 2012). This littoral lagoon covers a surface of 2,320 ha, characterized by an average depth of ca. 0.9 m and a maximum depth of

1.2 m (Soria 2006; IH Cantabria 2009). The lagoon is connected with the Mediterranean Sea through three channels called ‘golas’ (Pujol, Perelló and Perellonet) by means of sluice gates (see Figure 1) (Usaquén *et al.* 2012). The freshwater arriving to the Albufera comes from almost one hundred streams and irrigation channels and the precipitation-evaporation balance (Figure 2). The freshwater inflows, related to rice-growing, progressively decrease the salinity of the system (Rodrigo *et al.* 2010). Moreover, the lagoon is controlled by meteorological and astronomical tide and by wind.

Uni-dimensional models do not include the effect of geometry and bathymetry on mixing and circulation (Vidal *et al.* 2005). Here, we propose the application of a two-dimensional model to calculate tide-induced currents, inflows to the system, and the wind action. Once calibrated and validated, this type of model may produce high quality results. We present a two-dimensional long wave model coupled with a quasi-three-dimensional wind model including specifications on the opening and closing behaviour of the sluice gates through a discharge weir coefficient. On the one hand, the long wave model allows taking into account the tidal circulation (astronomical and meteorological), the flow discharged by the irrigation channels, the

balance between precipitation and evaporation and the inflows and outflows through the outlets (Bárcena *et al.* 2012; del Barrio *et al.* 2012). On the other hand, the wind model is used to calculate the wind induced circulation. The whole modelling system was calibrated and validated with real data from a whole hydrological year.

## THE HYDRODYNAMIC MODELS

Two hydrodynamic models developed by the Environmental Hydraulics Institute ‘IH Cantabria’ were used in this work. The first one, a two-dimensional depth-averaged model was used to characterize water circulation in the Albufera, the water fluxes entering the lagoon through the irrigation channels and those occurring through the three water outlets which connect the lagoon to the Mediterranean Sea. The second one, a quasi-three-dimensional model, was applied to calculate wind-induced currents in the lagoon and the coastal area. Wind modelling allows the vectorial coupling of hydrodynamics induced by wind with the currents obtained with the long wave model. In this simplified approach, the effects of both models are evaluated separately and then linearly summed. Specifically, currents in

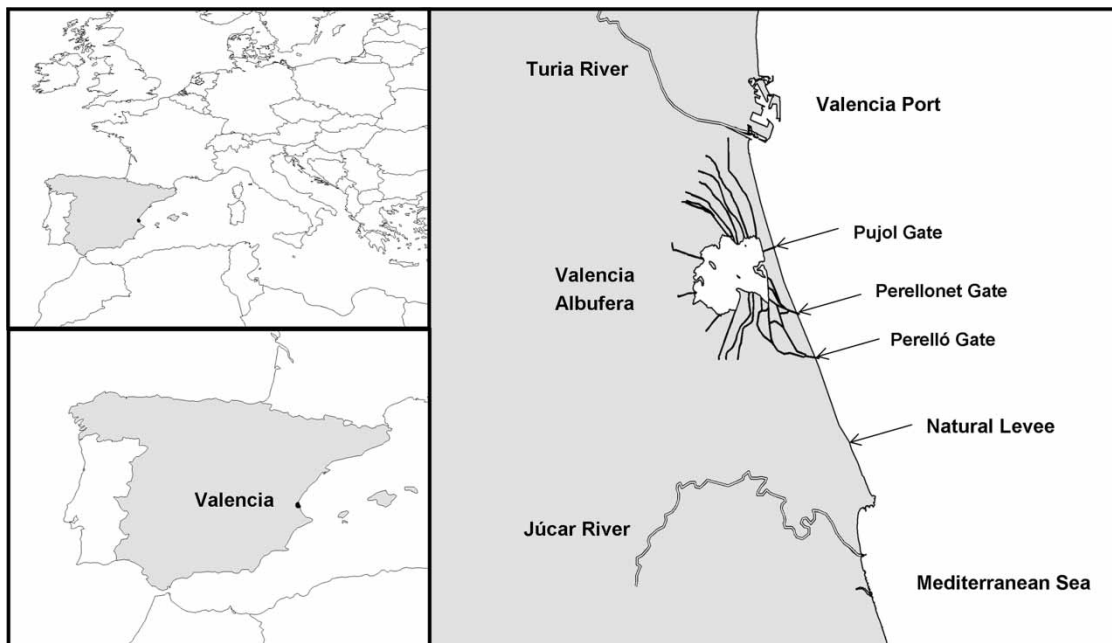


Figure 1 | Location of the study area.

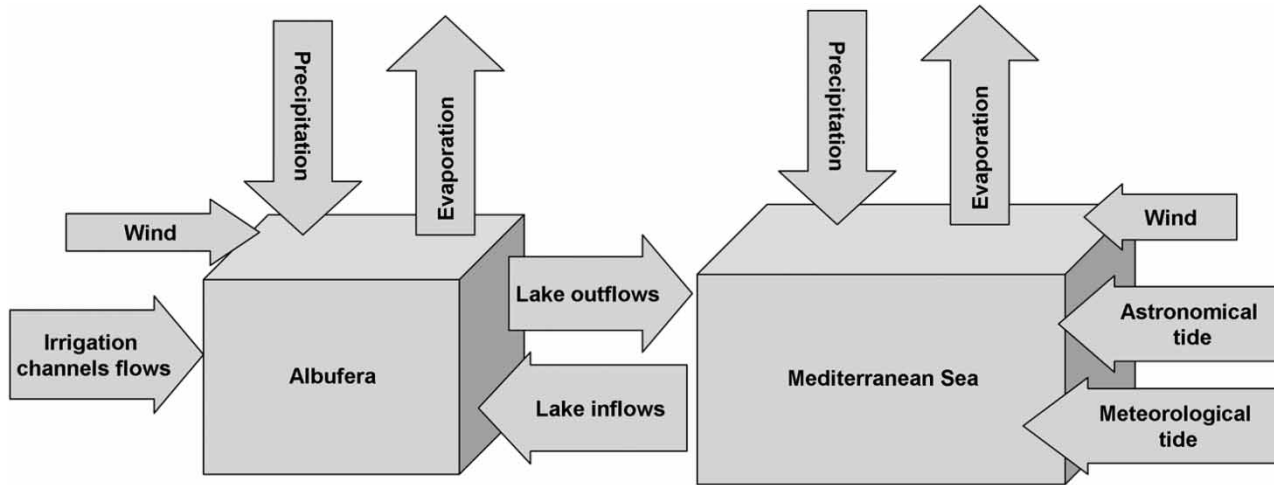


Figure 2 | Dynamic processes in the complex system of the Albufera of Valencia and the Mediterranean Sea.

the lagoon generated from ditch inflows and the sea-lagoon communication through the sluice gates are obtained using the long wave model. In turn, the wind model allows obtaining a parabolic velocity profile induced by the wind. This parabolic profile is integrated to obtain the current field in the water column due to the wind effect. These two fields of currents are linearly summed, to generate the global current field. The sea level variation in the lagoon is obtained using only the long wave model (the wind induced variations of the sea level are negligible). This approach has already been shown to provide good results in coastal lagoons and shallow waters (Koutitas 1988; Bombardelli & Menéndez et al. 2000; Johnson et al. 2005; Ding et al. 2006; Tsanis & Saied 2007; Haas & Warner 2009; Samaras & Koutitas 2012). As a consequence, it is not necessary to use three-dimensional models that usually involve many parameterizations and that also require a greater computational effort. Both models use the Alternating Direction Implicit (ADI) technique, to integrate the depth-averaged mass and momentum equations in the space-time domain.

**Long wave model**

The long wave model used here provides good results in shallow coastal areas (Castanedo et al. 2005; García et al. 2010a; Bárcena et al. 2012), as is the case of coastal lagoons. The computational code solves the depth-averaged three-dimensional Reynolds Averaged Navier-Stokes equations

dividing the study area into rectangular cells to calculate velocity and water surface elevation. The dimension of the cells is a function of the size of the study area, and its resolution depends on the desired level of detail. Governing motion equations are expressed as follows:

$$\frac{\partial UH}{\partial x} + \frac{\partial VH}{\partial y} + \frac{\partial H}{\partial t} = P - E \tag{1}$$

$$\begin{aligned} &\frac{\partial UH}{\partial t} + \frac{\partial(U^2H)}{\partial x} + \frac{\partial(UVH)}{\partial y} - fVH \\ &= -gH \frac{\partial \eta}{\partial x} - \frac{gH^2}{2\rho_o} \cdot \frac{\partial \rho_o}{\partial x} + N_x \left[ \frac{\partial^2(UH)}{\partial x^2} \right] + N_y \left[ \frac{\partial^2(UH)}{\partial y^2} \right] \\ &+ \frac{1}{\rho_o} (\tau_{sx} - \tau_{bx}) \end{aligned} \tag{2}$$

$$\begin{aligned} &\frac{\partial VH}{\partial t} + \frac{\partial(UVH)}{\partial x} + \frac{\partial(V^2H)}{\partial y} + fUH = -gH \frac{\partial \eta}{\partial y} - \frac{gH^2}{2\rho_o} \cdot \frac{\partial \rho_o}{\partial y} \\ &+ N_x \left[ \frac{\partial^2(VH)}{\partial x^2} \right] + N_y \left[ \frac{\partial^2(VH)}{\partial y^2} \right] + \frac{1}{\rho_o} (\tau_{sy} - \tau_{by}) \end{aligned} \tag{3}$$

where  $U$  and  $V$  are the components of depth-averaged velocities in the  $x$  and  $y$  directions,  $H$  is the water’s depth,  $g$  is the gravity constant,  $P-E$  is the balance between precipitation and evaporation,  $\eta$  is the water surface elevation from mean sea level,  $f$  is the Coriolis parameter,  $N_x$  and  $N_y$  are the horizontal eddy viscosity coefficients,  $\rho_o$  is the averaged density,  $\tau_{sx}, \tau_{sy}$  are the friction terms in the water

surface, and  $\tau_{bx}, \tau_{by}$  are the friction terms in the bed. We assumed that density was uniform in our simulations.

Water surface friction terms are expressed as a function of wind:

$$\frac{\tau_{sx}(\eta)}{\rho_o} = C_a \frac{\rho_a}{\rho_o} W_x \sqrt{W_x^2 + W_y^2} \quad (4)$$

$$\frac{\tau_{sy}(\eta)}{\rho_o} = C_a \frac{\rho_a}{\rho_o} W_y \sqrt{W_x^2 + W_y^2} \quad (5)$$

where  $C_a$  is a drag coefficient,  $\rho_a$  is the air's density, and  $W_x$  and  $W_y$  are the wind velocities in the  $x$  and  $y$  directions.

The bed friction terms are given by the following formulas:

$$\frac{\tau_{bx}(h)}{\rho_o} = \frac{gU\sqrt{U^2 + V^2}}{C^2H} \quad (6)$$

$$\frac{\tau_{by}(h)}{\rho_o} = \frac{gV\sqrt{U^2 + V^2}}{C^2H} \quad (7)$$

where  $C$  is the Chezy friction loss coefficient which can adopt different values depending on water depth as follows:

$$C = 18 \cdot \log\left(\frac{12 \cdot H}{K}\right) \quad (8)$$

where  $K$  is the Nikuradse roughness. Besides this formulation, the model also allows specification of a constant Chezy friction coefficient.

Following [Bárcena et al. \(2012\)](#), we implemented a wet-dry point treatment method in the model to simulate the wetting and drying processes for each cell in the tidal flat. This method introduces an additional bottom boundary layer and redefines the total water depth ( $D$ ) as  $H = H + h_c$ , where  $H$  is real total depth ( $H$ ) and  $h_c$  is the thickness of the bottom boundary layer. In terms of physics, the bottom boundary layer acts as a motionless viscous layer. Technically, this layer should be thin enough to satisfy a motionless condition thereby ensuring numerical stability ([Zheng et al. 2003](#)). If  $D$  is larger than  $h_c$ , the point is treated as a wet point and its velocity and elevation are computed

from the finite-difference equations. Otherwise it remains a dry point where water velocity is equal to zero. The thickness of the critical layer used was 10 cm, based on sensitivity studies of velocity and tidal elevation to  $h_c$ .

Since the model considers the effect of precipitation and evaporation to define the mass balance equation, daily precipitation and evaporation regimes in  $\text{mm d}^{-1}$  were specified as input data. Based on this information, the model assesses the water balance at each time step, increasing or decreasing the free surface level. Moreover, we modelled the connection between the lagoon and the sea through the 'golas', which are controlled by several gates. The effect of these hydraulic structures on the lagoon's discharge was included in the long wave model using the following weir discharge equation ([Idelchik 1996](#)):

$$Q = \left(\frac{2}{3}\right)^{3/2} C_g \cdot b \cdot g^{1/2} \left(h_1 + \frac{U_1^2}{2g}\right)^{3/2} \quad (9)$$

where  $C_g$  is a discharge coefficient which has to be calibrated,  $b$  is the weir's width,  $g$  is the gravity constant,  $U_1$  is the upstream velocity,  $h_1$  is the height of the free surface above the weir, and  $Q$  is the resulting flow passing through the gate. In this way, the gate regulatory effect on the water flux has been taken into account by an overflow weir discharge. ADI is an implicit method, which does two scannings (in the  $x$  and  $y$  directions) of the equation on the domain at the same time (implicit point of view). However, the time increment between different time steps has to keep a Courant number  $< 1$  due to stability criteria. Before the second scanning, the model solves the additional equation to obtain  $Q$  at the 'golas'.

The time step for the hydrodynamic model was chosen to be 6 s to ensure stable conditions according to Courant criteria. A constant eddy viscosity coefficient ( $E$ ) of  $0.1 \text{ m}^2 \text{ s}^{-1}$  was estimated by means of the formula ([Álvarez 1996](#)):

$$E = K \cdot \Delta x \cdot U_{\text{characteristic}} \quad (10)$$

where  $K$  is a parameter between 0.05 to 0.15,  $\Delta x$  is the cell size and  $U_{\text{characteristic}}$  is a characteristic velocity of the domain. At open boundaries, the water levels and

freshwater flows were prescribed. At the open sea boundary, the tidal elevation from the Andersen-Grenoble version 95.1 model (Le Provost 2001) was used. The irrigation channel inputs were introduced in the model as river flow conditions (Figure 3(b)). An initial condition of zero metres above mean sea level was considered to start the simulation.

### Wind model

Wind currents have a different vertical pattern to tidal velocities or inflows and outflows. The wind moves the water mainly on the surface, while near the bottom its effect is generally negligible. Thus, we used a quasi-three-dimensional model which takes into account the different structure of

horizontal velocities due to wind action as a function of depth (Koutitas 1988). This model provided good results in shallow coastal areas (García et al. 2010b). Its governing equations are the following:

$$\frac{\partial UH}{\partial x} + \frac{\partial VH}{\partial y} + \frac{\partial H}{\partial t} = 0 \quad (11)$$

$$\begin{aligned} \frac{\partial U}{\partial t} + U \frac{\partial U}{\partial x} + V \frac{\partial U}{\partial y} + \left(0.2U + \frac{a_x}{40}\right) \frac{\partial U}{\partial x} \\ + \left(0.2V + \frac{a_y}{40}\right) \frac{\partial U}{\partial y} = -g \frac{\partial \eta}{\partial x} + fV \\ + \frac{\tau_{sx}}{\rho_0 H} - \left(0.18 \frac{U}{H} \sqrt{\frac{\tau_{sx}}{\rho_0}} - 0.5 \frac{\tau_{sx}}{\rho_0 H}\right) \end{aligned} \quad (12)$$

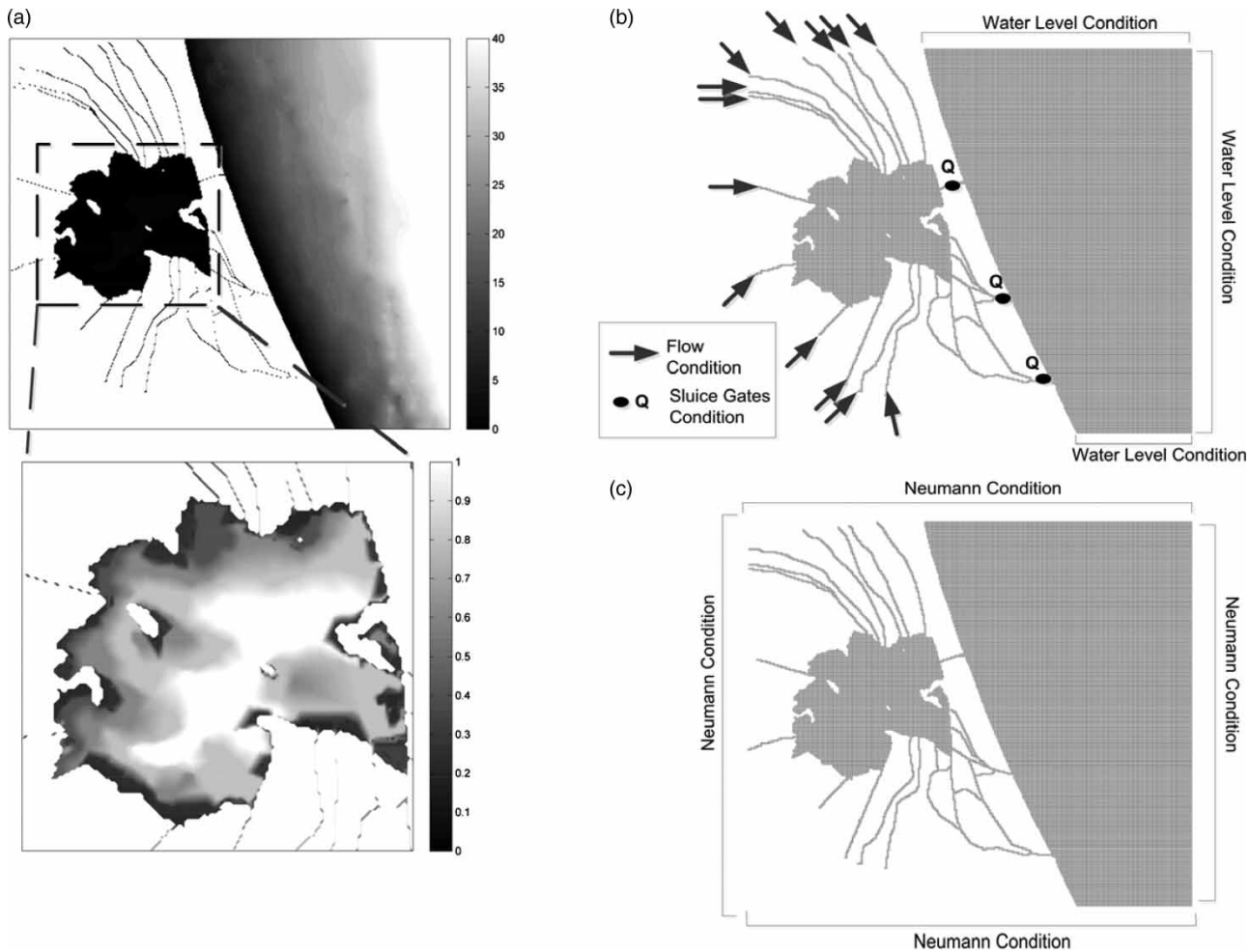


**Figure 3** | (a) Hydrodynamic model grid of the whole aquatic system (irrigation channels, lagoon, 'golas' and Mediterranean Sea). (b) Boundary conditions of long wave model. (c) Boundary conditions of wind model.

$$\begin{aligned} \frac{\partial V}{\partial t} + U \frac{\partial V}{\partial x} + V \frac{\partial V}{\partial y} + \left(0.2U + \frac{a_x}{40}\right) \frac{\partial V}{\partial x} \\ + \left(0.2V + \frac{a_y}{40}\right) \frac{\partial V}{\partial y} = -g \frac{\partial \eta}{\partial x} - fU \\ + \frac{\tau_{sy}}{\rho_0 H} - \left(0.18 \frac{V}{H} \sqrt{\frac{\tau_{sy}}{\rho_0}} - 0.5 \frac{\tau_{sy}}{\rho_0 H}\right) \end{aligned} \quad (13)$$

where  $\tau_{sx}, \tau_{sy}$  are the friction terms in the water surface (calculated with the same method as the long wave model) and  $a_x$  and  $a_y$  are coefficients obtained from the parabolic approach of the velocity profile in the  $x$  and  $y$  direction described as:

$$a_x = 16.6 \sqrt{\frac{\tau_{sx}}{\rho_0}} \quad (14)$$

$$a_y = 16.6 \sqrt{\frac{\tau_{sy}}{\rho_0}} \quad (15)$$

The wind model used an ADI method. To obtain stable results according to Courant criteria, we selected a time step of 6 seconds. Additionally, a drag coefficient of 0.0026 was selected for the wind model (García et al. 2010b). In this model, all boundaries were considered as open boundaries under Neumann conditions (Figure 3(c)). As with the long wave model, an initial condition of zero metres above mean sea level was considered to start the simulation.

### The numerical grid

Both hydrodynamic models were applied over the same numerical grid. This grid consisted of  $345 \times 300$  square cells with a cell dimension of 50.0 m (see Figure 3(a)), which is sufficiently fine to model the hydrodynamics of the coastal lagoon. Bathymetric data were taken from detailed topographic works (one data point each 50 m) developed for the entire Albufera Park (TYPSA Group 2004; Universidad Politécnica de Valencia 2009) and the navigation charts of the State's Naval Hydrographic Institute (numbers 47, 48, 474, 481, 482 and 791). Based on this information, an interpolation technique ('kriging' method) was used to obtain the grid shown in Figure 3. This numerical grid includes the irrigation channels that discharge into the lagoon, the lagoon itself, its connection to

the sea through the three 'golas' (which constitute a complex set of channels equipped with sluice gates) and the coastal area. Figure 3 also shows the shallowness of the lagoon with maximum depths above 1 metre only at its central area.

## FORCING EFFECTS ON LAGOON CIRCULATION

The simulations have been carried out considering the effect of different forcings (tide, wind, irrigation channel contributions, evaporation-precipitation balance and sluice gates opening regime) on water lagoon circulation.

Astronomical tide characteristics at the study area are described in Table 1. The low amplitude of the tidal components led to a small variation of the sea water surface with a maximum tidal range of 25 cm (Figure 4(a)). Meteorological tides cause changes in coastal areas as a result of pressure variations and wind. To obtain the meteorological tide, water surface levels, measured at a tidal gauge of the Spanish National Port Administration located inside Valencia's harbour, were used. The surface water variation caused by the meteorological tide is shown in Figure 4(b). Based on this approach, a record of sea level variations was obtained integrating the astronomical and meteorological tide contributions every 600 s throughout the study period (October 2005 to September 2006) (Figure 4(c)). Furthermore, wind was characterized from data measured at a meteorological station of the Automatic Hydrological Information System located at Picassent (6.3 km north of

**Table 1** | Astronomical tidal components (Component), amplitude ( $A_i$ ) and phase ( $\psi_i$ ) of tidal wave harmonic components for the coastal area of Valencia

Component	$A_i$ (m)	$\psi_i$ (°)
SA	0.064	252.74
SSA	0.036	56.78
MSM	0.042	350.29
MM	0.013	241.51
O1	0.025	107.89
P1	0.012	143.27
S1	0.011	249.29
K1	0.037	159.73
M2	0.018	194.37

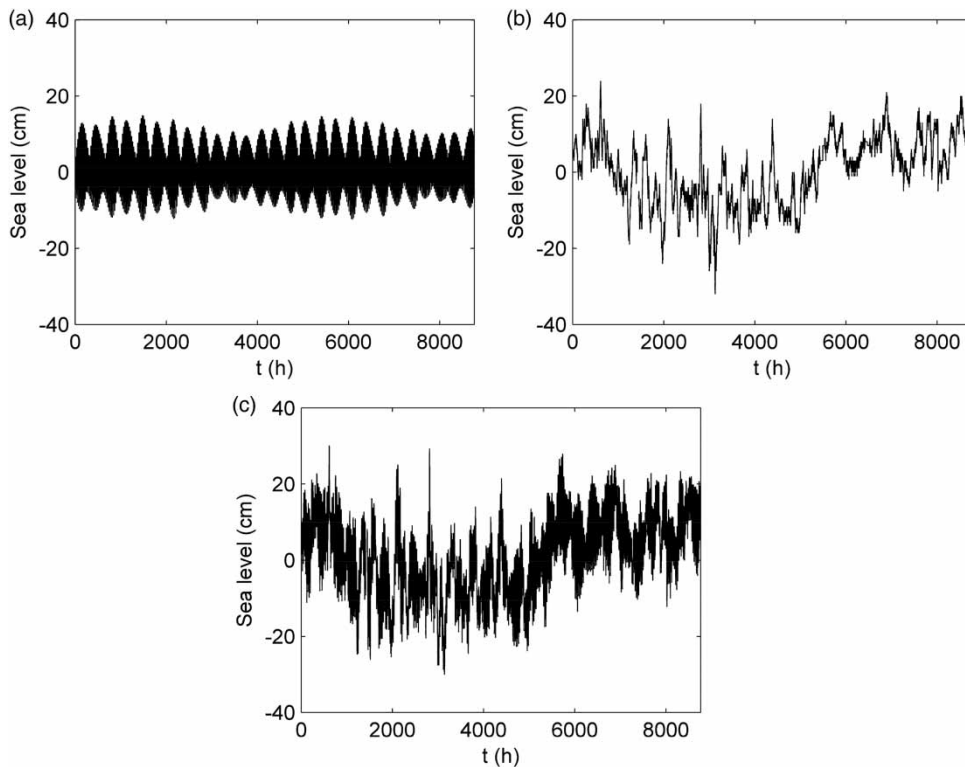


**Figure 4** | Water surface variation in the period October 2005 to September 2006 caused by: (a) astronomical tide; (b) meteorological tide; (c) both astronomical and meteorological tides.

Albufera). The data analysis of the main wind events is shown in Figure 5. A secondary forcing is the precipitation-evaporation balance. Daily average precipitation and evaporation data were obtained from the series measured at Picassent's meteorological station. Evaporation was lower in winter with a minimum value of  $0.43 \text{ mm d}^{-1}$  and higher in summer with a maximum value of  $7.67 \text{ mm d}^{-1}$ . During the study period, the total annual evaporation was 357.8 mm, while the annual precipitation was 1,110.2 mm. Precipitation was concentrated mainly in autumn and winter and was scarce during the summer. The maximum daily precipitation was 36.8 mm, while a total of 93 rainy days were registered.

An important forcing for water circulation in the Albufera is the input of over 60 irrigation ditches. Due to the difficulty in taking field measurements and working with such a high number of channels, only 13 major ditches were selected (IH Cantabria 2009). Daily flow discharges of these 13 ditches were obtained from different monitoring stations belonging to the National Water

Authority (Confederación Hidrográfica del Júcar 2009) between 2005 and 2009. These ditches were chosen because of their importance in terms of water flow. Therefore, the whole contribution of flow discharges to the lagoon was distributed over these 13 channels. Figure 6 shows the maximum, minimum and mean daily flow values of the irrigation channel discharges into the lagoon during the period between October 2005 and September 2006.

As mentioned before, the Albufera is connected to the sea by three 'golas' (Pujol, Perelló and Perellonet), where water flow is regulated by means of 27 sluice gates, distributed as follows: 11 gates at Pujol channel, 7 at Perellonet and the remaining 9 located at the Perelló gola. Since 2005, the Valencia City Council has managed the operation of the sluice gates. The sluice gates located at the Pujol 'gola' are the ones which are open more often (161 days), followed by those at the Perelló 'gola' (141 days) and finally the Perellonet 'gola' ones (107 days). Most of the time less than half of the gates are only partially open, the opening time being

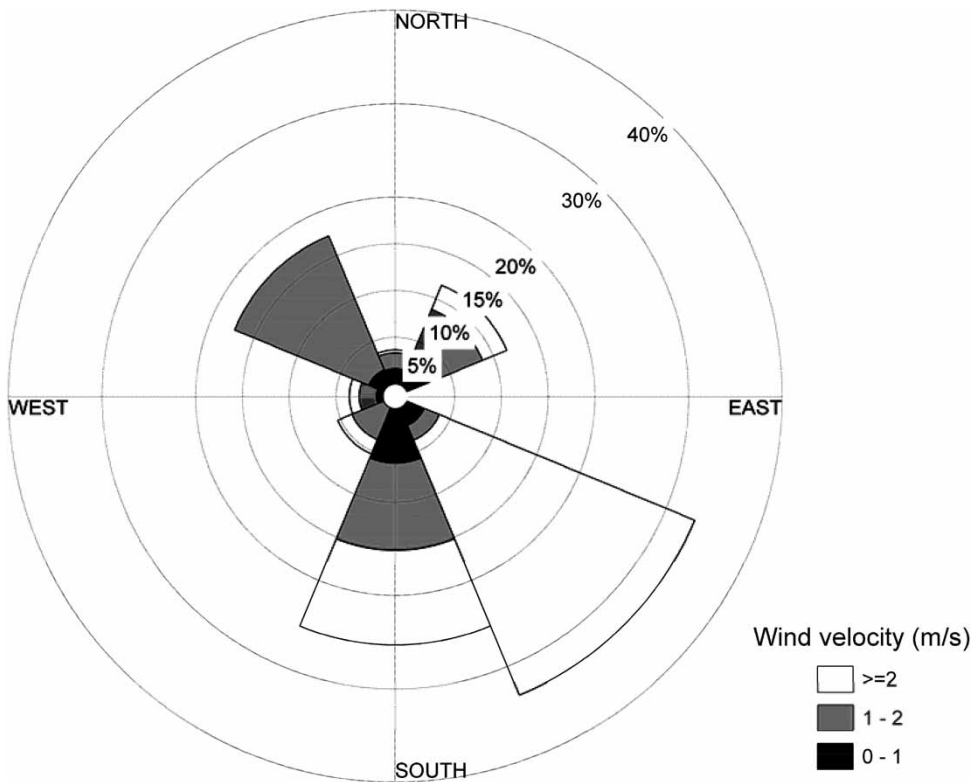


**Figure 5** | Wind rose at Picassent meteorological station in the period 2001–2009.

mainly at the end of the autumn and during the winter season. The gates are completely closed during the months of July and August.

## HYDRODYNAMIC MODEL ASSESSMENT

The complexity of the whole aquatic system of the Valencia Albufera led us to consider a different analysis to calibrate and validate the hydrodynamic models. Thus, three studies were carried out focusing on the following aspects: calibration of the bottom friction and eddy viscosity coefficients, calibration of the discharge coefficient  $C_g$ , and validation of the whole hydrodynamic modelling from an analysis of the lagoon's behaviour. Calibration of the long wave model parameters was carried out based on sea water level variation in the coastal area. Definition of the  $C_g$  coefficient was made by comparing the model predictions with the water levels and flows measured at the sluice gates. For the last study, the lagoon levels were

used in order to validate the results obtained with the hydrodynamic models.

## Long wave model parameter calibration

The long wave hydrodynamic model was calibrated with surface water elevation data measured by the tidal gauge located at the Port of Valencia. The calibration was performed by comparing the model predictions and the data collected throughout the study period (October 2005 to September 2006). This comparison allowed the establishment of a Nikuradse roughness ( $K$ ) of 0.2 m and an eddy viscosity coefficient of  $0.1 \text{ m}^2 \text{ s}^{-1}$ . Figure 7 shows how a good agreement was achieved between modelled and observed sea water levels. Not only was the trend reproduced but so were the water levels. The Nash-Sutcliffe coefficient of efficiency ( $CE$ ) (Nash & Sutcliffe 1970) obtained a value of 0.99, which can be considered excellent, while the mean relative error ( $E_r$ ) was equal to 1.8%, which according to Thomann & Mueller (1987) makes the model's predictions reliable.



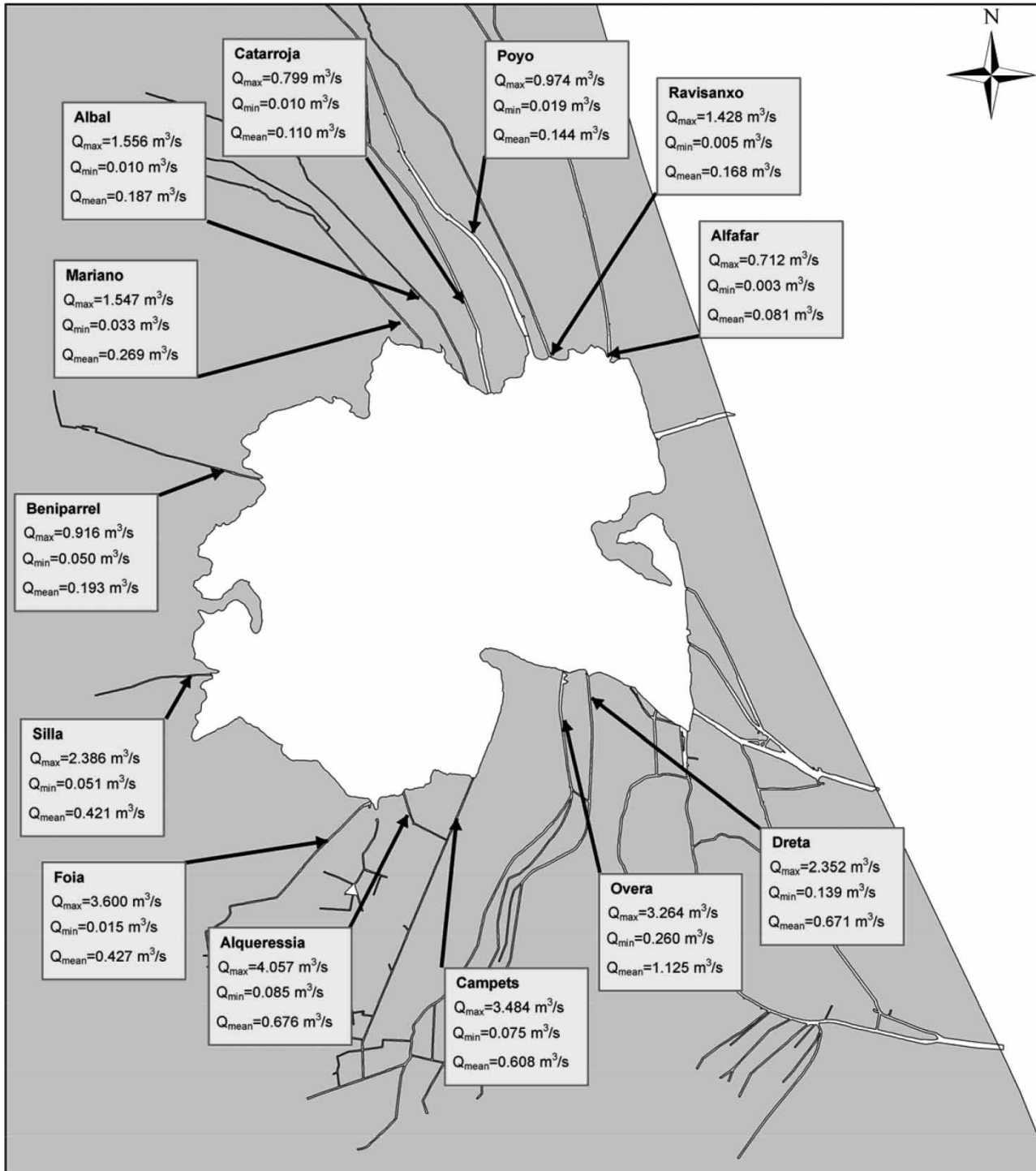
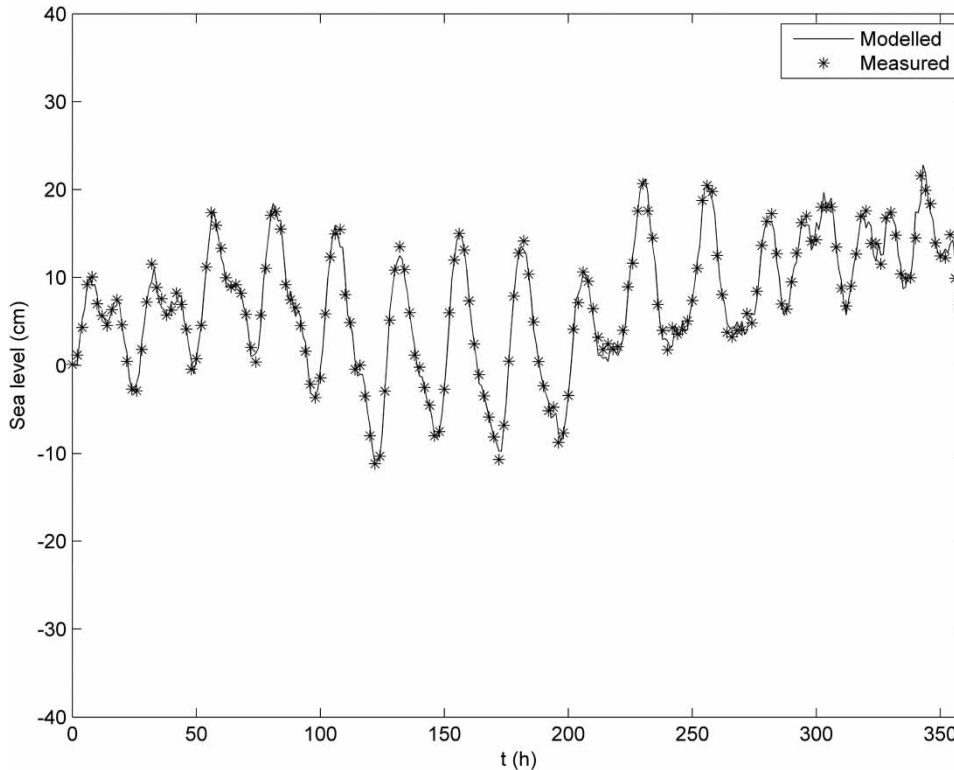


Figure 6 | Maximum, minimum and mean value of irrigation channel discharges into the lagoon from October 2005 to September 2006.



**Figure 7** | Comparison between modelled and measured sea water surface levels during the period between November 1st and November 15th, 2005.

### Assessment of the discharge coefficient $C_g$

As described before, a new parameter was introduced in the long wave model to take into account the effect of the sluice gate system on the flow evacuated through the 'golas'. In this way, the discharged flow was related to the number of open sluice gates through the discharge coefficient  $C_g$ . To estimate this coefficient, time periods in which only the Pujol 'gola' was opened were used. These periods were the following: (i) May 28th, 2006–May 30th, 2006 for a single sluice gate open; (ii) November 8th, 2005–November 10th, 2005 for two to four sluice gates open; (iii) September 1st, 2006–September 3rd, 2006 for calibration when four to seven sluice gates were opened; and (iv) December 25th, 2005–December 27th, 2005 when eight to 11 sluice gates allowed evacuation of lagoon water. The calibration was conducted by comparing results predicted by the model with lagoon water levels and flows measured at the Pujol 'gola' location during those periods. Table 2 shows those values obtained for the discharge coefficient  $C_g$  which showed the best fit.

**Table 2** | Discharge coefficient ( $C_g$ ) values as a function of the number of opened sluice gates, including relative errors ( $E_r$ ) for level and flow predictions

Number of sluice gates	$E_r$ in level prediction (%)	$E_r$ in flow prediction (%)	$C_g$
1	0.1	2.1	0.2
2–4	0.1	3.7	0.3
4–7	0.3	2.4	0.4
8–11	0.5	5.3	0.5

This table also shows the relative error ( $E_r$ ) found in the simulated lagoon level and discharged flow with respect to the data provided by the National Water Authority (Confederación Hidrográfica del Júcar 2009).

### Hydrodynamic model validation at the Albufera lagoon

The validation process focused on the comparison of modelled water levels with measurements obtained during the study period (October 2005–November 2006). The lagoon's water levels were obtained from a buoy installed by the

National Water Authority (*Confederación Hidrográfica del Júcar 2009*) at the Pujol 'gola'. Simulated water levels were obtained taking into consideration the contribution of the two hydrodynamic models. The long wave model was used to consider the effect of daily irrigation discharge flows, the daily balance of precipitation and evaporation, the water circulation and sea surface levels caused by tides in the coastal area, as well as the resulting inflows or outflows through the 'golas'. The wind model was used to calculate water currents and surface level variations inside the lagoon and in the coastal zone, considering hourly wind episodes.

The lagoon water levels predicted from both models have been added at the buoy location. *Figure 8* shows how the modelled predictions of water level at the buoy reproduce the trends observed. The *CE* showed a value of 0.55, which can be considered good for a validation process (*Nash & Sutcliffe 1970*). The mean relative error ( $E_r$ ) was 15.7%, indicating a reasonable prediction of water level variations (*Usaquén et al. 2012*).

## MODEL RESULTS AND DISCUSSION

Two hydrodynamic models were applied to the Albufera's aquatic system considering the October 2005–September 2006 period. To analyse the effect of each forcing circulation, hourly velocity currents were calculated. The annual averaged velocities induced by the interaction among the inputs from the irrigation channels, the evaporation-precipitation balance and the outputs through the 'golas' are shown in *Figure 9(a)*. This figure shows how the maximum

velocities were concentrated near the mouth of the main contribution channels (Overa, Dreta, Campets and Alqueressia) and close to the three 'golas', with maximum velocities of  $0.02 \text{ m s}^{-1}$ . However, due to the fact that inflows from the irrigation channels are a tiny portion of the lagoon's volume, currents in the central part are practically negligible. Moreover, the lagoon acts as a water reservoir for almost half of the year. This fact can be seen in *Figure 8*, which shows a high water level increase during several periods.

The annual averaged currents caused by wind action are presented in *Figure 9(b)* showing that the circulation in the entire lagoon is strongly affected by wind, which increases inflow mixing with maximum wind-induced currents of about  $0.02 \text{ m s}^{-1}$ . Wind generates a shore current along the north and south areas of the lagoon. The average velocity pattern shows four large vortexes (see *Figure 9(b)*) located at: (i) the vicinity of the north shore; (ii) the area of the Perelló and Perellonet 'golas'; (iii) the southern shore near the Campets irrigation channel mouth; and (iv) the central area of the lagoon, with lower maximum velocity values.

The global water circulation movement was obtained by summing long wave and wind models results. The lagoon's global circulation (*Figure 9(c)*) shows that annual average velocities are in general dominated by wind-generated currents. Only in areas closest to the 'golas' and in the southeastern part of the lagoon are the wind currents slightly modified by inflows-outflows induced dynamics. Clearly, this is the main advantage of the proposed model over other models previously applied to the Albufera (*Usaquén et al. 2012*), since the latter did not provide information about velocity patterns in the lagoon area. Moreover,

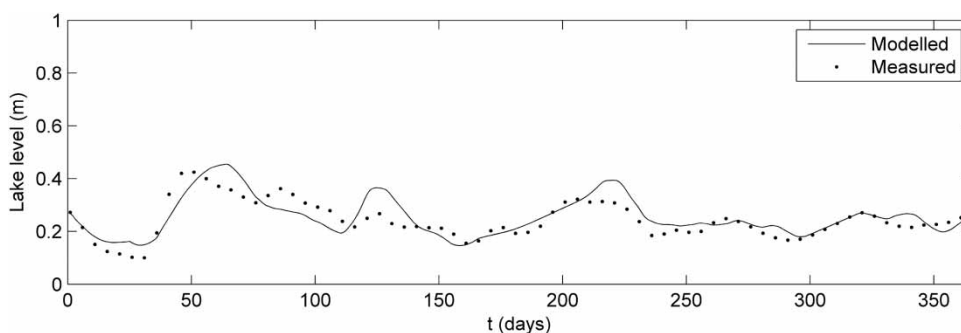


**Figure 8** | Comparison between computed and measured lagoon surface water level from October 2005 to September 2006.

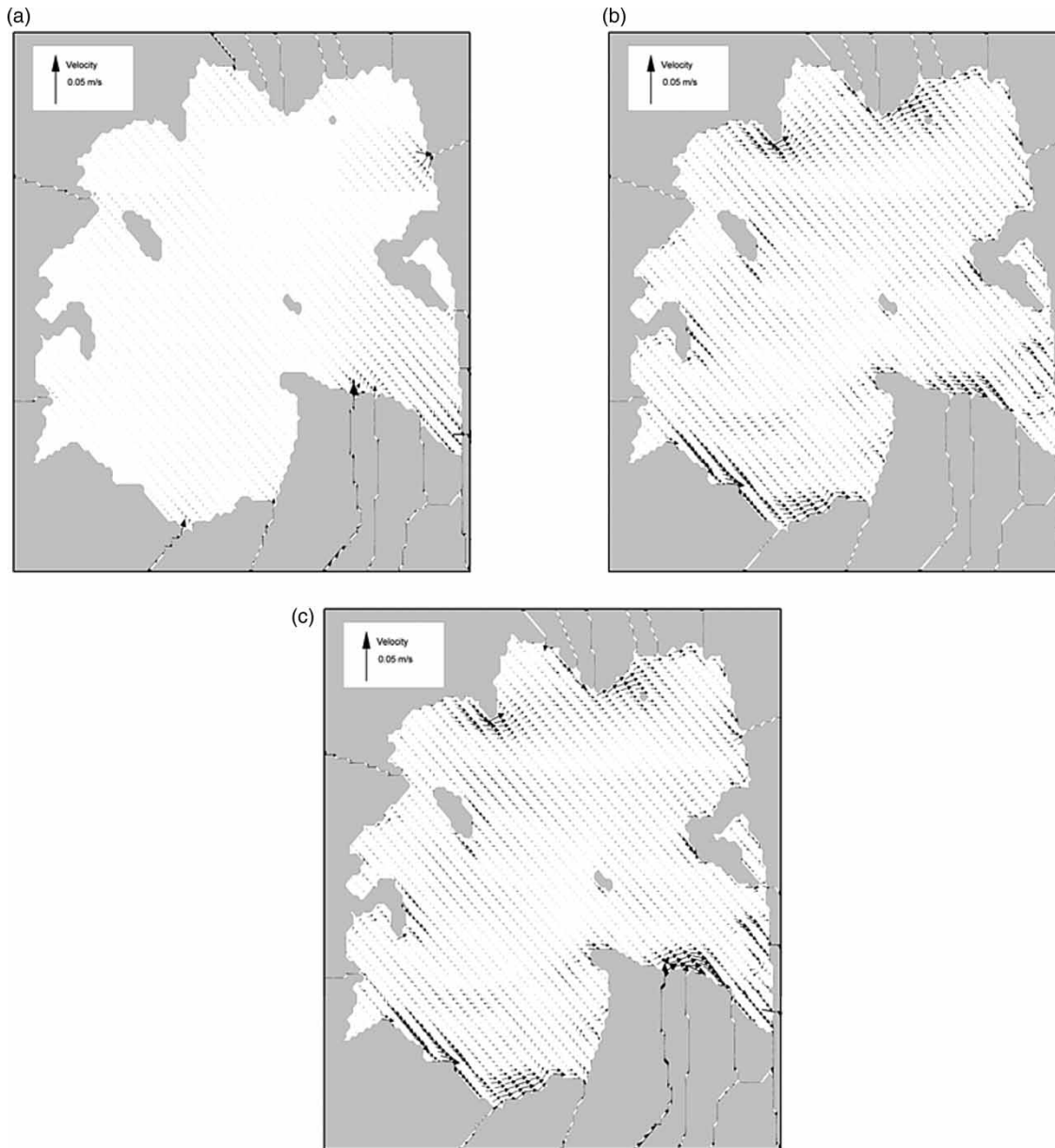


**Figure 9** | Average annual circulation patterns of (a) long wave model currents, (b) wind model field currents and (c) global field currents.

coupling this two-dimensional hydrodynamics model with a water quality model allows the spatial assessment of pollutant transport and eutrophication in the lagoon (del Barrio *et al.* 2012), which is not possible with one-dimensional models. In this sense, the two-dimensional modelling results directly provide information regarding those areas of the Albufera of Valencia with higher and lower renovation rates, respectively.

We also conducted a comparison of the modelled lagoon outflows with observed data at the Pujol 'gola'. As shown in Figure 10, results of the model present a good efficiency ( $CE = 0.73$ ) and reliable correlations with the data ( $r^2 = 0.76$ ). The total discharged water volume obtained with the model was  $41.1 \times 10^6 \text{ m}^3$  which shows a good agreement with a measured value of  $48.1 \times 10^6 \text{ m}^3$ . These results show that the model is able to adequately describe the

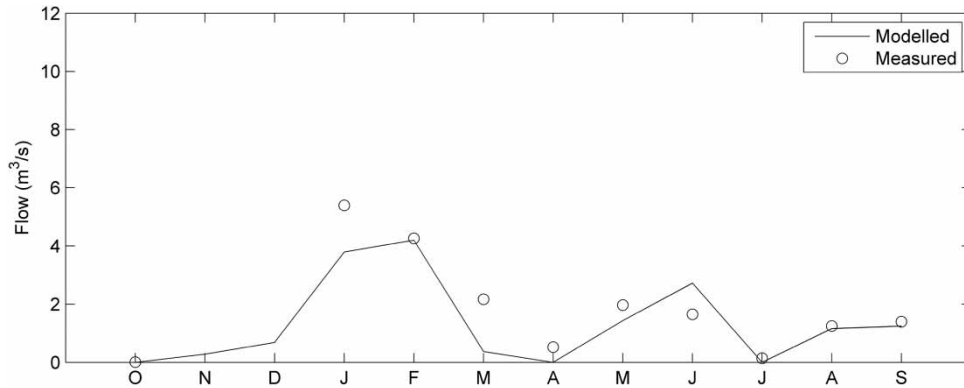


**Figure 10** | Comparison of modelled and measured monthly mean flows at the Pujol 'gola'.

flow discharge through the gates. Connection of semi-confined water bodies to the sea has generally been treated as a boundary condition in two-dimensional modelling (Salles *et al.* 2005; Spillman *et al.* 2009). Here, we modelled the lagoon-sea connection inner domain by means of an overflow weir discharge, describing the hydrodynamic behaviour of the system on both sides of the 'golas'. This

allowed evaluation of the effect of lagoon outflow on coastal currents. It is important to highlight the great benefit obtained over one-dimensional models that can only assess the net bidirectional flux but not its spatial distribution in the domain.

The annual distribution of the daily outflow at the gate location from model results is shown in Figure 11, the

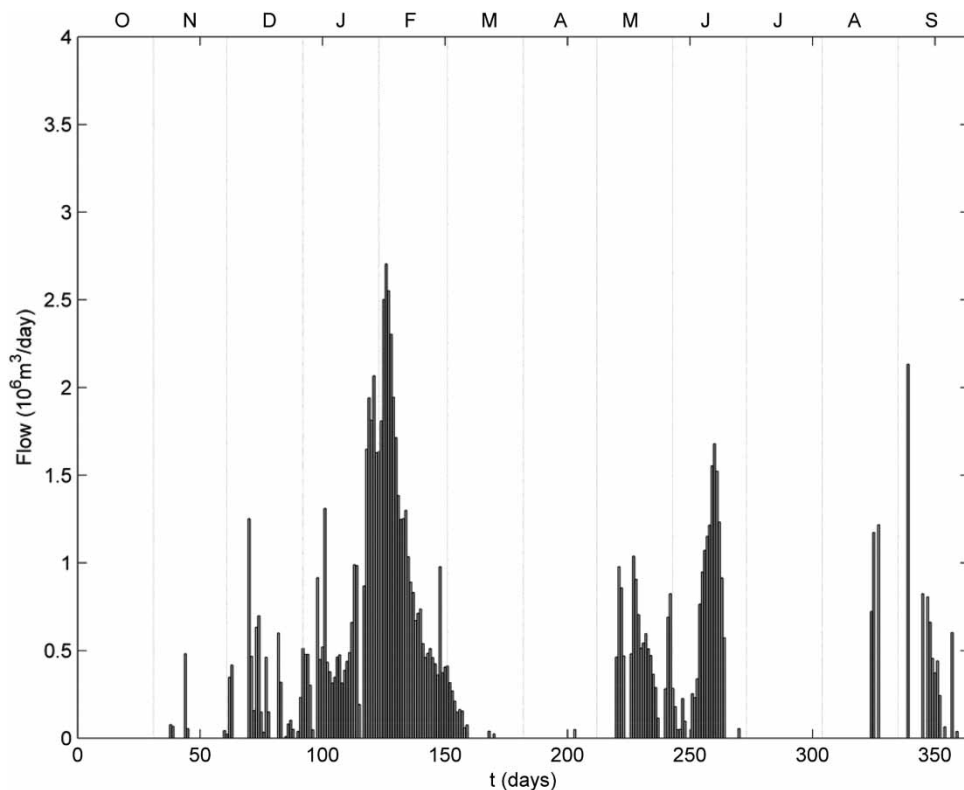


**Figure 11** | Daily lagoon outflows through the sluice gates.

total annual outflow in the study period being  $98.1 \times 10^6 \text{ m}^3$ . Figure 11 also shows that flow increases between January and February coinciding with the drainage of rice fields prior to seeding, which takes place in April (Vicente & Miracle 1992; Romo *et al.* 2007). In May and June, an increase in the outflows was observed, which was associated with a partial discharge at the time of crop development. Finally, in September, the emptying of the rice fields for the harvest produced another flow discharge period.

## SUMMARY AND CONCLUSIONS

We carried out a hydrodynamic modelling to characterize the water level and flow velocities in a complex regulated lagoon using a two-dimensional depth-averaged long wave model and a quasi-three-dimensional wind model. The overall circulation pattern was established by adding the velocity fields provided by each hydrodynamic model. We considered different hydrodynamic forcings to characterize global water circulation in the system: irrigation channel contributions, meteorological and astronomical tides, precipitation-evaporation balance and the wind effect. In addition to these forcings, the effect of sluice gate management at the 'golas' connecting the lagoon with the sea was also included through the implementation of a discharge weir equation. These effects on lagoon water level and salinity were introduced in the long wave model code as an additional formulation. We used a discharge coefficient as a calibration parameter to regulate the flow through the 'golas'. The discharge weir coefficient varied between 0.2 and 0.5 for a proper description of sluice gates opening.

A 1-year time period was used for hydrodynamic model validation. The comparison of modelled and observed lagoon water levels showed a good agreement. Thus, the integration of both models allowed the assessment of flow patterns in the selected study area. Moreover, the lagoon outflows provided by the hydrodynamic modelling system reproduced the observed trend leading to a good fit in terms of *CE*. The obtained outflows were directly related to rice farming which is in agreement with several research studies (Roselló 1979; del Barrio *et al.* 2012). Therefore, the present model contributes to a better understanding of coastal lagoon hydrodynamics where the sea connection is

highly regulated, with the application and assessment of new formulas for the opening and closing regime of a system of sluice gates.

## ACKNOWLEDGMENTS

This study was funded by the National Plan I + D + i (2012) of the Spanish Ministry of Science and Innovation (Project CTM2012-32538) and the Entidad Pública de Saneamiento de Aguas de Valencia. We are grateful to Giovanni Coco for helpful comments and recommendations.

## REFERENCES

- Álvarez, C. 1996 Aportaciones metodológicas al estudio de la contaminación litoral originada por vertidos y alivios procedentes de redes de saneamiento urbano. PhD Thesis. Universidad de Cantabria.
- Bárcena, J. F., García, A., García, J., Álvarez, C. & Revilla, J. A. 2012 Surface analysis of free surface and velocity to changes in river flow and tidal amplitude on a shallow mesotidal estuary: an application in Suances Estuary (Northern Spain). *Journal of Hydrology* **420-421**, 301-318.
- Bombardelli, F. A. & Menéndez, A. N. 2000 *Un modelo cuasi-tridimensional para corrientes inducidas por el viento en aguas poco profundas*. XIX Congreso Latino Americano de Hidráulica, Córdoba.
- Castanedo, S., Medina, R., Losada, I., Vidal, C., Méndez, F., Osorio, A., Juanes, J. A. & Puente, A. 2005 The Prestige oil spill in Cantabria (Bay of Biscay). Part I: operational forecasting system for quick response, risk assessment, and protection of natural resources. *Journal of Coastal Research* **22**, 272-287.
- Confederación Hidrográfica del Júcar 2009 *Conducción Júcar-Vinalopó*. Ministry of Environment, Spain.
- del Barrio, P., García, A., García, J., Álvarez, C. & Revilla, J. A. 2012 A model for describing the eutrophication in a heavily regulated coastal lagoon. Application to the Albufera of Valencia (Spain). *Journal of Environmental Management* **112**, 340-352.
- Ding, Y., Wang, S. Y. & Jia, Y. 2006 Development and validation of a quasi-three-dimensional coastal area morphological model. *Journal of Waterway, Port, Coastal and Ocean Engineering* **132**, 462-476.
- García, A., Juanes, J. A., Álvarez, C., Revilla, J. A. & Medina, R. 2010a Assessment of the response of a shallow-macrotidal estuary to changes in hydrological and wastewater inputs through numerical modelling. *Ecological Modelling* **221**, 1194-1208.

- García, A., Sámano, M. L., Juanes, J. A., Medina, R., Revilla, J. A. & Álvarez, C. 2010b [Assessment of the effects of a port expansion on algae appearance in a coastal bay through mathematical modelling. Application to San Lorenzo Bay \(North Spain\)](#). *Ecological Modelling* **221**, 1413–1426.
- Haas, K. A. & Warner, J. C. 2009 [Comparing a quasi-3D to a full 3D nearshore circulation model: SHORECIRC and ROMS](#). *Ocean Modelling* **26**, 91–103.
- Idelchik, I. E. 1996 *Handbook of Hydraulic Resistance*. Begell House, New York.
- IH Cantabria 2009 *Estudio de los efectos del saneamiento sobre las aguas de l'Albufera*. Santander.
- Johnson, H. K., Karambas, T. V., Avgeris, I., Zanuttigh, B., Gonzalez-Marco, D. & Caceres, I. 2005 [Modelling of waves and currents around submerged breakwaters](#). *Coastal Engineering* **52** (10–11), 949–969.
- Koutitas, C. G. 1988 *Mathematical Models in Coastal Engineering*. Pentech Press, London.
- Le Provost, C. 2001 Ocean Tides. In: *Satellite Altimetry and Earth Sciences: A Handbook of Techniques and Applications* (L. Fu & A. Cazenave, eds). Academic Press, San Diego, 463 pp.
- Li, M., Gargett, A. & Denman, K. 1999 [Seasonal and interannual variability of estuarine circulation in a box model of the Strait of Georgia and Juan de Fuca Strait](#). *Atmosphere-Ocean* **37**, 1–19.
- Liang, S. J. & Molkenthin, F. 2001 [A virtual GIS-based hydrodynamic model system for Tamshui River](#). *Journal of Hydroinformatics* **3** (4), 195–202.
- Murray, A. G. & Parslow, J. S. 1999 [The analysis of alternative formulations in a simple model of a coastal ecosystem](#). *Ecological Modelling* **119**, 149–166.
- Nash, J. E. & Sutcliffe, J. V. 1970 [River flow forecasting through conceptual models part I – A discussion of principles](#). *Journal of Hydrology* **10**, 282–290.
- Pasarić, M. & Orlic, M. 2001 [Long-term meteorological preconditioning of the North Adriatic coastal floods](#). *Continental Shelf Research* **21** (3), 263–278.
- Rodrigo, M. A., Alonso-Guillén, J. L. & Soulié-Märsche, I. 2010 [Reconstruction of the former charophyte community out of the fructifications identified in Albufera de València lagoon sediments](#). *Aquatic Botany* **92** (1), 14–22.
- Romo, S., García-Murcia, A., Villena, M. J., Sánchez, V. & Ballester, A. 2007 [Tendencias del fitoplancton en el lago de la Albufera de Valencia e implicaciones para su ecología, gestión y recuperación](#). *Limnetica* **27** (1), 11–28.
- Roselló, V. M. 1979 [Els espais albuferencs del País Valencià](#). *Acta Geològica Hispànica* **14**, 487–493.
- Salles, P., Voulgaris, G. & Aubrey, D. G. 2005 [Contribution of nonlinear mechanisms in the persistence of multiple tidal inlet systems](#). *Estuarine, Coastal and Shelf Science* **65** (3), 475–491.
- Samaras, A. G. & Koutitas, C. G. 2012 [An integrated approach to quantify the impact of watershed management on coastal morphology](#). *Ocean & Coastal Management* **69**, 68–77.
- Soria, J. M. 2006 [Past, present and future of the Albufera of Valencia Natural Park](#). *Limnetica* **25**, 135–142.
- Spillman, C. M., Hamilton, D. P. & Imberger, J. 2009 [Management strategies to optimise sustainable clam \(\*Tapes philippinarum\*\) harvest in Barbamarco Lagoon, Italy](#). *Estuarine, Coastal and Shelf Science* **81** (2), 267–278.
- Thomann, R. V. & Mueller, J. A. 1987 *Principles of Surface Water Quality Modeling and Control*. Harper & Row, Pub., Inc., New York.
- Tsanis, I. K. & Saied, U. 2007 [A wind-driven hydrodynamic and pollutant transport model](#). *Global NEST Journal* **9** (2), 117–131.
- TYPSA Group 2004 *Clasificación y Organización Cartográfica*. Valencia.
- Universidad Politécnica de Valencia 2009 *Batimetría de acequias y golas de l'Albufera*. Valencia.
- Usaquén, O. L., Gómez, A. G., García, A. & Álvarez, C. 2012 [Methodology to assess sustainable management of water resources in coastal lagoons with agricultural uses: an application to the Albufera lagoon of Valencia \(Eastern Spain\)](#). *Ecological Indicators* **13** (1), 129–143.
- Vicente, E. & Miracle, M. R. 1992 [The coastal lagoon Albufera de Valencia: an ecosystem under stress](#). *Limnetica* **8**, 87–100.
- Vidal, J. P., Moisan, S., Faure, J. B. & Dartus, D. 2005 [Towards a reasoned 1D river model calibration](#). *Journal of Hydroinformatics* **7** (2), 91–104.
- Zheng, L., Chen, C. & Liu, H. 2003 [A modeling study of the Satilla River estuary, Georgia. I: Flooding-drying process and water exchange over the salt marsh estuary shelf complex](#). *Estuaries* **26**, 651–669.

First received 31 May 2013; accepted in revised form 2 February 2014. Available online 22 February 2014